Physics Letters B 782 (2018) 112–116

Contents lists available at ScienceDirect

Physics Letters B

www.elsevier.com/locate/physletb

First measurement of the isoscalar excitation above the neutron emission threshold of the Pygmy Dipole Resonance in ^{68}Ni

N.S. Martorana [a,b,*], G. Cardella [c], E.G. Lanza [c], L. Acosta [d,c], M.V. Andrés [e], L. Auditore [f,c], F. Catara [c], E. De Filippo [c], S. De Luca [f,c], D. Dell' Aquila [g], B. Gnoffo [b,c], G. Lanzalone [h,a], I. Lombardo [c], C. Maiolino [c], S. Norella [f,c], A. Pagano [c], E.V. Pagano [a], M. Papa [c], S. Pirrone [c], G. Politi [b,c], L. Quattrocchi [c], F. Rizzo [a,b], P. Russotto [a], D. Santonocito [c], A. Trifirò [f,c], M. Trimarchi [f,c], M. Vigilante [g], A. Vitturi [i]

[a] INFN-LNS, Catania, Italy
[b] Dipartimento di Fisica e Astronomia, Università degli Studi di Catania, Catania, Italy
[c] INFN-Sezione di Catania, Catania, Italy
[d] Instituto de Fisica, Universidad Nacional Autonoma de Mexico, Mexico City, Mexico
[e] Departamento de FAMN, Universidad de Sevilla, Sevilla, Spain
[f] Dipartimento MIFT, Messina, Italy
[g] INFN-Sezione di Napoli and Dipartimento di Fisica, Università di Napoli Federico II, Napoli, Italy
[h] Facoltà di Ingegneria e Architettura, Università Kore, Enna, Italy
[i] Dipartimento di Fisica e Astronomia, Università G. Galilei and INFN-Sezione di Padova, Padova, Italy

ARTICLE INFO

Article history:
Received 23 January 2018
Received in revised form 7 May 2018
Accepted 8 May 2018
Available online 16 May 2018
Editor: V. Metag

Keywords:
Pygmy Dipole Resonance
Unstable nuclei
Isoscalar probe

ABSTRACT

The excitation of the Pygmy Dipole Resonance (PDR) in the ^{68}Ni nucleus, above the neutron emission threshold, via an isoscalar probe has been observed for the first time. The excitation has been produced in reactions where a ^{68}Ni beam, obtained by the fragmentation of a ^{70}Zn primary beam at INFN-LNS, impinged on a ^{12}C target. The γ-ray decay was detected using the CsI(Tl) detectors of the CHIMERA multidetector sphere. The ^{68}Ni isotope as well as other heavy ion fragments were detected using the FARCOS array. The population of the PDR was evidenced by comparing the detected γ-ray energy spectra with statistical code calculations. The isotopic resolution of the detection system allows also to directly compare neutron decay channels with the ^{68}Ni channel, better evidencing the PDR decay response function. This comparison allows also the extraction of the PDR cross section and the relative γ-ray angular distribution. The measured γ-ray angular distribution confirms the E1 character of the transition. The γ decay cross section for the excitation of the PDR was measured to be 0.32 mb with a 18% of statistical error.

1. Introduction

Recently, much relevance has been given to the collective states in neutron-rich nuclei. The remarkable interest in these states is also driven by the presence of an electric dipole response around the nucleon binding energy [1–3]. This mode, the so-called Pygmy Dipole Resonance (PDR), although is carrying few per cent of the isovector dipole Energy Weighted Sum Rule (EWSR), has been predicted to be present in all the nuclei with neutron excess; in particular for those far from the stability line. In a pioneering work [4], it has been shown that, as soon as the number of neutrons increases, the isovector and isoscalar dipole responses show a small bump at low energy in the strength distribution, which is well separated from the well known peak of the Giant Dipole Resonance (GDR). This mode has a strong relation with the symmetry energy and it has been used as a further tool to constrain it [5,6]. Furthermore, the PDR might have a big influence on the astrophysical r-process nucleo-synthesis, since the presence of an even small dipole strength around the neutron separation energy strongly enhances the neutron capture cross sections [7–9].

Assuming that a nucleus with a neutron excess is formed by a saturated core, with the same number of neutrons and protons,

* Corresponding author at: Università degli Studi di Catania and INFN-LNS, Via Santa Sofia, 62, Catania, Italy.
E-mail address: martorana@lns.infn.it (N.S. Martorana).

https://doi.org/10.1016/j.physletb.2018.05.019

and a neutron skin, the PDR can be considered as a surface mode associated with the motion of the neutron skin against the saturated core. Several microscopic many body models [1,10–16] are able to describe the low-lying dipole strength, and they all agree on the properties of the transition densities: the neutrons and protons transition densities are in phase inside the nucleus but at the surface just the neutron part, with opposite phase, survives. These properties give rise to a transition density where the isovector and isoscalar character are mixed, and therefore this mode can be populated by both isoscalar and isovector probes [15].

Several experiments have been performed on stable nuclei [1–3]. The comparison between the excitation of these low dipole states induced by either alpha particles, ^{17}O nuclei or real photons reveals a particular property which is known as "isospin splitting" [2,3,17–25]: only the low energy region of the PDR is populated by both isoscalar and isovector probes, while the higher part is excited mainly via electromagnetic interaction. This sharp separation of pure isovector and mixed isoscalar-isovector states, in a very limited energy range, has to be better understood and it is currently a topic of interest [26,27]. Until now the isospin splitting has been observed for almost all the stable nuclei analyzed. It is interesting to investigate whether the same effect is present also for the PDR region above the neutron emission threshold and for unstable nuclei. The experimental study of the PDR at an energy above the neutron emission threshold, with unstable nuclei, has been done in pioneering experiments, carried out at the GSI, using relativistic Coulomb excitations on ^{132}Sn [28] and ^{68}Ni [29,30] isotopes. The presence of the PDR in unstable nuclei was investigated using relativistic Coulomb excitations also in refs. [31–33].

In this work, we report on the first observation of the PDR, above the neutron emission threshold, in the ^{68}Ni nucleus, using an isoscalar probe, obtained in an experiment carried out at INFN-LNS of Catania. In order to excite the PDR we used an isoscalar target of ^{12}C. Semiclassical calculations, based on microscopic form factor built with microscopic RPA transition densities [14–16] show that, at the energy used (28 A MeV), most of the total inelastic PDR cross section (more than 60%) is due to the pure nuclear interaction. The Coulomb contribution amounts at 9%, while another 30% is given by the interference between nuclear and Coulomb contributions. Such calculations have been done according to the semiclassical model described in [13–15], where the real part of the optical potential has been obtained by the double folding procedure, while the imaginary part has been chosen to have the same geometry of the real part with half of its intensity. This is a kind of standard procedure when one has no experimental information about the elastic scattering cross section.

2. Experiment

In Fig. 1 a sketch not to scale of the experimental apparatus is presented. A ^{70}Zn primary beam was accelerated to an energy of 40 A MeV, using the Superconducting Cyclotron (CS), and it impinged on a 250 µm thick ^{9}Be target to produce, with a projectile fragmentation reaction, the ^{68}Ni beam, delivered via the FRIBs@LNS fragment separator of the INFN-LNS [34,35]. In such a facility, a tagging system was used in order to event by event characterize the cocktail beam [36]. A large surface Micro-Channel Plate (MCP) gives the *start* of the Time of Flight (ToF) measurement of the beam. The *stop* of the ToF is delivered by a Double-Sided Silicon Strip Detector (DSSSD), with 32 × 32 strips 2 mm width, and 156 µm thick, placed at about 12.9 m from the MCP, along the transport beam line, approximately 2 m before the ^{12}C reaction target. The DSSSD provides also the energy loss information for the ΔE–ToF identification method, moreover the DSSSD produces also the first information on the beam position to measure

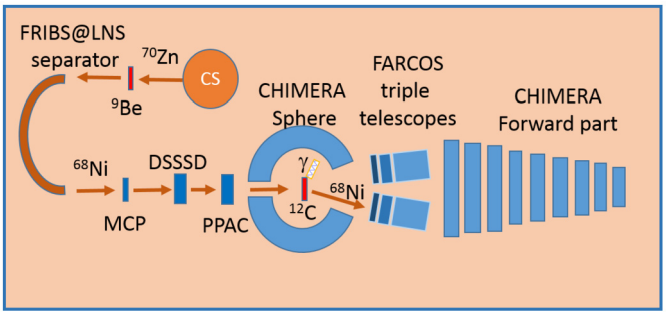

Fig. 1. Sketch, not to scale, of the used experimental set up (color online).

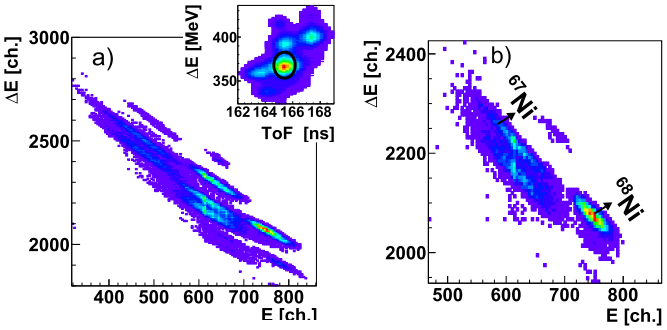

Fig. 2. a) ΔE–E scatter plot observed with the FARCOS array irradiated by the reactions products produced with the whole cocktail fragmentation beam. Isotopic identification of fragments with Z from 27 to 30 is observed. In the inset the ΔE–ToF identification scatter plot of the cocktail beam is reported. b) Reaction products detected with the FARCOS array in coincidence with ^{68}Ni ions, as shown in the black circle in the inset of Fig. 2a (color online).

the trajectory. The second position information was provided by a Parallel Plate Avalanche Counter (PPAC) device, mounted at about 80 cm from the target, and having 1 mm spatial resolution. A ^{12}C target, 75 µm thick, was used to induce the isoscalar excitation on the projectile nucleus. The scattered ^{68}Ni ions were detected and identified in four prototype telescopes of the FARCOS array [37,38]. During the experiment the FARCOS array was placed just after the sphere of the CHIMERA multidetector [39,40] and it covered angles from 2° to 7°, with approximately 70% coverage of azimuthal angles. The FARCOS modules are triple telescopes, each of them constituted by two stages of DSSSD 300 and 1500 µm thick, followed by four CsI(Tl) scintillators read by a photo-diode. ^{68}Ni scattered ions were stopped in the second stage of the telescopes.

3. Analysis and results

As above mentioned, we used the tagging system to get event by event the isotopic composition of the exotic beam. In the inset of Fig. 2a is reported the ΔE–ToF plot obtained with this tagging system. The ^{68}Ni beam, evidenced by the black circle, is the most intense beam in the cocktail (about 20% of the total intensity). The beam energy, after the DSSSD detector, is about 28 A MeV. At this beam energy the ion identification is difficult because of the presence of not fully stripped ions produced after the ^{9}Be target. Just the 92% of the incoming Zn beam is totally stripped, more than the 7% of the ions have a charge status of 29^{+}, and also the 28^{+} charge status is present. However, the configuration of the transport beam line, with the presence of magnets after the MCP, allows to reject the largest amount of this background by the stripping effect of the mylar foil. With this method we were therefore able to correctly identify the $^{68}Ni^{28+}$ beam. A more quantitative analysis

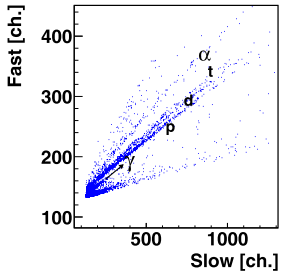

Fig. 3. Pulse shape discrimination plot in a CsI(Tl) detector of the CHIMERA sphere. We note that only light particles and γ-rays are observed due to the forward focusing of the reaction products (color online).

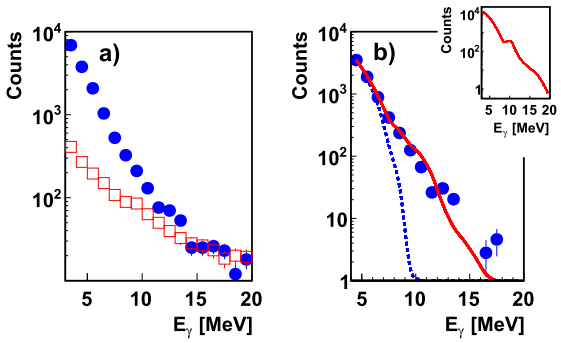

Fig. 4. a) The blue dots represent the γ-ray energy spectrum, Doppler shift corrected, in coincidence with Ni fragments detected by the FARCOS array (Fig. 2b). The red squares represent the background. b) γ-ray spectrum (blue dots) obtained by subtracting the two spectra shown in Fig. 4a. The blue dashed line is the γ-ray energy spectrum produced by the ^{68}Ni statistical decay, folded with the detector response function, obtained using the standard CASCADE code. The red continuous line is the CASCADE calculation, folded with the detector response function, by including the presence of the PDR, GDR and the GQR. In the inset the CASCADE calculation by including the presence of the PDR, the GDR and the GQR, without the folding, is reported (color online).

of the contamination of tagged beams will be discussed in the following. The high quality of the FARCOS silicon detectors response, together with the cleaning effect of the fragment separator, allows the full isotopic identification of ^{68}Ni, as it is shown in Fig. 2a. In Fig. 2b it is shown the ΔE–E plot, obtained with the FARCOS array, in coincidence with the ^{68}Ni beam, shown as a black circle in the inset of Fig. 2a. From the Fig. 2 b one can better appreciate the amount of the contamination of the tagged beam by $^{66}Ni^{27+}$ (14%) produced at similar energy with respect to the one of the main beam. A second contaminant of lower intensity (7%) is $^{66}Cu^{28+}$ produced at lower beam energy. Thanks to the isotopic resolution of the detection system, and to the energy difference of the various nuclei, reaction products generated by these contaminants can be easily removed.

The PDR can decay both by neutron or by γ-ray emission (the last one with lower probability). In order to detect γ-rays we used the second stage of the telescopes of the CHIMERA multidetector sphere, composed of CsI(Tl) scintillators read by a photo-diode. Details on the γ-rays detection and identification can be found in refs. [41,42]. The energy calibration of CsI(Tl) detectors was performed using 24 MeV proton elastic and inelastic scattering on ^{12}C, ^{197}Au and CH_2 targets. More in detail scattering of protons and pulser signals were used to calibrate all detectors in proton equivalent energy, verifying the linearity of the response function. The proton energy calibration was converted in γ-ray energy calibration using, as a reference point, the γ-ray from the decay of the 4.44 MeV level of the ^{12}C. These γ-rays provided also a check for the angular distribution and efficiency calibration, as shown in [42]. The p + ^{12}C collision was also useful in order to verify that the probability to produce γ-rays from the decay of excited ^{12}C is negligible in the region around 10 MeV, where the PDR is expected. All excited levels in this energy range have in fact a negligible γ-decay branching ratio [43].

In order to identify the γ-rays, we used the so called fast-slow method described in [41]. In Fig. 3 an example of pulse shape discrimination plot, obtained in this experiment, is shown. The timing of the MCP was used as a reference time for the pulse shape analysis.

Due to the large energy spread of the fragmentation beam (2%), it is difficult from ion energy measurements to evaluate the total kinetic energy loss and from this to extract the average excitation energy of the system. However, as it was seen in Fig. 2b, ^{68}Ni + ^{12}C reactions mostly produce, at forward angles, two kind of reactions: reactions in which the mass of ^{68}Ni projectile does not change, and reactions in which one or two neutrons are emitted and ^{66,67}Ni ions are detected. The elastic channel is not observed due to the FARCOS angular coverage; the grazing angle is in fact around 0.7°. In Fig. 4a we report, as blue dots, the γ-ray energy spectrum, Doppler shift corrected by assuming an emission by the projectile, and measured in coincidence with the Ni fragments detected by the FARCOS array (Fig. 2b). We note the presence of γ-rays yield extending up to 20 MeV. However, the most energetic γ-rays detected are essentially due to spurious coincidences. This background has been evaluated moving the fast-slow cuts on both sides around the γ line and it is plotted as red squares. The difference between the coincidence spectrum and the background is reported as blue dots in Fig. 4b. In order to evidence the population of the PDR, in this figure, are also reported two calculations performed using the statistical code DCASCADE [44,45]. The blue dashed line is obtained with a standard statistical calculation, while the red full line includes the strength due to the population of the PDR, the standard GDR and the Giant Quadrupole Resonance (GQR). The population of the Isoscalar Giant Monopole Resonance (ISGMR) and Isoscalar Giant Quadrupole Resonance (ISGQR) have been studied in the ^{68}Ni in refs. [46,47]. At the energy of 28 A MeV, the cross section for the population of the ISGMR is very low and moreover this mode can not decay, at least at the ground state, by γ-rays emission; for these reasons we neglected this transition in the CASCADE calculation. Whereas, we included in the statistical calculation also the presence of the GQR, by considering the values reported in refs. [46,47]. We also underline that while resonances must be explicitly inserted, standard accepted constant strengths of other transitions are included in CASCADE.

The statistical calculations reported in Fig. 4b were performed assuming a range of excitation energies with a maximum at 26.5 MeV. The range of excitation energies has been fixed in order to reproduce the charge distribution observed (Fig. 2b) and the slope of the spectrum from 2 to 6 MeV. Excitation energies larger than 28 MeV are excluded because we do not detect mass smaller than 66. The blue dashed line statistical calculation reproduces just the first region of the spectrum (from 2 to 6 MeV), in fact, due to the competition of particle emission , if no resonance is excited, the high energy γ-decay probability is very small. The experimental spectrum is reproduced only including resonances and in particular we inserted in the CASCADE calculation a PDR contribution with a centroid around 10 MeV, a width of 2 MeV and a strength of 9% $\pm$ 2% EWSR, a GDR contribution with a centroid of 17 MeV, a width of 6 MeV and a strength of 91% $\pm$ 2% EWSR and a GQR with a centroid around 16 MeV and a width of 1.5 MeV.

The parameters of the PDR and GDR resonances are in reasonable agreement, inside our errors bars, with the values reported in ref. [30]. These statistical calculations are folded with the CsI(Tl) response function, evaluated by performing Geant4 [48,49] simula-

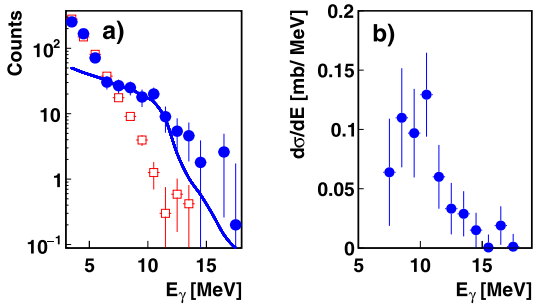

Fig. 5. a) γ-ray energy spectra Doppler shift corrected. The blue dots represent the coincidence with ^{68}Ni. The red squares represent the γ-ray energy spectrum in coincidence with ^{66,67}Ni. These spectra have been normalized at low energy. The blue full line is the γ-rays first step spectrum obtained with CASCADE (see text). b) Cross section of the PDR obtained with the subtraction of the spectra shown in Fig. 5a (color online).

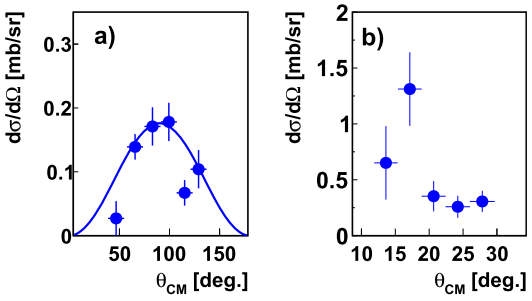

Fig. 6. a) The measured γ-ray angular distribution. The line is the expected E1 angular distribution. b) The ^{68}Ni angular distribution measured in coincidence with γ-rays in the region of the pygmy resonance (color online).

tion. In order to better understand the effect of the folding procedure, in the inset of Fig. 4b is reported the statistical calculation by including the PDR, the GDR and the GQR, without the folding with the CsI(Tl) response function. There, one can clearly see the bump corresponding to the excitation of the low-lying dipole state.

Due to the energy resolution of CsI(Tl) detectors the population of the PDR in Fig. 4b is evidenced only by a small change of slope around 10 MeV and by the comparison with statistical calculations. A better experimental evidence of the PDR population can be obtained by comparing the γ energy spectra measured in coincidence with the ^{68}Ni channel and ^{66,67}Ni channels. In fact, at this low excitation energy the high energy γ-decay of the PDR hinders further particle decay. On the contrary, if one or more neutrons are emitted by the system, the high energy γ-rays decay is inhibited.

For these reasons we compare in Fig. 5a the γ-rays energy spectrum (blue dots) in coincidence with the ^{68}Ni (Fig. 2b), with the one measured in coincidence with neutron decay channels ^{66,67}Ni. The two spectra are normalized in the low energy region. Also these spectra are Doppler shift corrected by assuming an emission from the projectile. The background was evaluated and subtracted with the fast-slow cuts, as shown in Fig. 4a. We note in Fig. 5a the enhancement around 10 MeV, as it was expected, due to the PDR decay in the ^{68}Ni channel. We observe a relatively small yield in the GDR high energy region as predicted by the semiclassical calculations. Indeed, these calculations show that, at these relatively low incident energies and with the low Coulomb field of the target, the excitation probability for the PDR mode is higher than the one corresponding to the GDR energy region. The small yield is however also due to the lower detection efficiency in the higher energy region. We underline that it is not possible to compare the exclusive energy spectra of Fig. 5 with inclusive CASCADE calculations. However, one can compare the γ-rays spectrum in coincidence with ^{68}Ni with γ-rays first step spectra generated with CASCADE, namely with the γ-rays emitted as first particle in the decay process. In fact, such events at the low excitation energy of the system produce only ^{68}Ni nuclei. This calculation, folded with the CsI(Tl) response function, is plotted as blue full line in Fig. 5a. The comparison is quite good and the calculation reproduces the bump in the energy region of the PDR. Clearly, in this calculation, the lower energy spectrum is not reproduced because in this energy region the contribution of the decay of discrete levels in the final decay steps is missing.

In Fig. 5b we report the PDR energy γ-spectrum obtained by subtracting the two normalized spectra of Fig. 5a. This method allows to give a lower limit to the PDR yield, because some small PDR contribution could be present also in the ^{66,67}Ni coincidence spectrum. However this is the simplest way to compare the PDR yield with previous experimental results [29] and look to the presence of isospin splitting above particle emission threshold. The cross section is obtained taking into account the detection efficiency, as better specified in the following. It is very important to verify the E1 character of the observed bump at around 10 MeV in coincidence with the ^{68}Ni channel, in order to prove the dipole character of the transition. To prove this we extracted the angular distribution of the emitted γ-rays in the region of the enhancement at around 10 MeV shown in Fig. 5b. The granularity of the spherical region of the CHIMERA multidetector, covering angles from 30° to 176°, in step of 8° up to 146°, allows to extract the angular distribution. Because of the relatively low statistics, we were forced to sum γ-rays detected in two rings of the apparatus; therefore the effective laboratory angular resolution was ±8°, being negligible the error in the evaluation of the ^{68}Ni scattering angle assumed as reference axis. This angular distribution is shown in Fig. 6a. Notwithstanding the scarce statistics, the angular distribution shows the typical distribution expected for a dipole transition with a maximum around 90° (full blue line). The angular distribution was corrected for the effective γ-ray detection efficiency evaluated using Geant4 simulation at 10 MeV, taking into account the thickness of CsI(Tl) scintillators of the sphere (from 8 to 4 cm) mounted at different angles and malfunctioning detectors. On average the total γ-ray detection efficiency was of the order of 25%. In order to evaluate the overall detection efficiency it is also important to determine the angular distribution of the emitted ^{68}Ni in coincidence with the PDR enhancement. Unfortunately, due to losses in efficiency of the PPAC detector we did not have the information on the beam trajectory for all the events. However, the beam divergence was rather low, of the order of 0.5°; therefore by assuming this error in the angular distribution (and a further 0.2° due to the angular straggling in the thick ^{12}C target), and correcting for the average beam direction that can be evaluated by the impinging position in the DSSSD detector, we were able to evaluate the angular distribution which is plotted in Fig. 6b. We note that the largest part of the events is collected from 12° to 20°, with a maximum around 15° in the CM reference frame. The overall beam efficiency was calculated with a Monte-Carlo simulation, by using the measured beam distribution. Taking into account the observed angular distribution, one can evaluate an average efficiency for the ^{68}Ni detection of the order of 52%.

We can not extract much more physical information from the ^{68}Ni angular distribution, shown in Fig. 6b. In fact, to perform meaningful DWBA calculations we should also have the measured elastic scattering angular distribution in order to fix the optical potential. However, the ^{68}Ni angular distribution is important for evaluating the ^{68}Ni detection efficiency and it may be a reference point for future measurements.

The absolute cross sections of the pygmy γ-ray decay reported in Fig. 5b, Fig. 6a and Fig. 6b are obtained thanks to the event by

event counting of the beam intensity and the knowledge of target thickness, once determined the detection efficiency. In total, we counted about 1.4×10^9 ^{68}Ni beam particles. Taking into account the average beam detection efficiency (52%) and the average γ-ray detection efficiency (25%), the total cross section of the PDR γ-decay amounts at 0.32 mb with a statistical error of the order of 18%.

Being sure of the E1 character of the resonance we can compare the measured γ-ray spectrum to the one obtained using an almost pure isovector probe, like in the relativistic Coulomb excitation in ref. [29]. Comparing our results with the results obtained in ref. [29] there is almost an order of magnitude difference between the two cross sections, which is probably caused by the different reactions regimes. Furthermore, in the GSI experiment [29] the maximum of the strength distribution is located at around 11 MeV, while in this case it seems peaked at around 10 MeV, more in agreement with the result obtained in ref. [30]. Due to the response function of CsI(Tl) detectors, the enhancement observed at 10 MeV is generated by γ-rays with energy of approximately 10.5 MeV. The different slope of statistical γ-ray spectra underlying the resonance and propagation errors, in the calibration procedure, can account for the residual difference on the observed energy strength of the resonance. Within the small statistics and the relatively scarce energy resolution of the present measurement and previous experiments [29,30], this comparison seems to indicate that the outcome of the excitation process due to the two isoscalar and isovector probes is similar along the PDR energy region. Therefore the isospin splitting seems not to be observed at the energy above the neutron emission threshold; however more precise measurements are necessary to better prove this observation.

4. Conclusions

In summary we have observed, for the first time, the γ-ray decay of the pygmy resonance populated by an isoscalar probe in the ^{68}Ni. The measured γ-ray angular distribution shows the E1 character of the resonance. The measured cross section of the process amounts at 0.32 mb with 18% of statistical error. We have shown that ^{12}C is a good probe for the isoscalar excitation. Moreover, the target contribution to the γ-ray energy spectrum in the region around 10 MeV is negligible. We have also shown that the E1 states at the low lying energy region around 10 MeV can be excited by both isoscalar and isovector probes which is in agreement with the theoretical findings [16] about the mixed character of these dipole states. From the comparison with previous experiments performed with isovector probes it seems that the so-called isospin splitting is not present for the low lying dipole states found at excitation energies above the neutron emission threshold. However, due to the limits of the relative small statistics and relative scarce energy resolution of the present measurement and previous experiments [29,30], it is not possible to draw definite conclusions. Moreover, the role of multistep contributions to the population of the PDR, which is not present in the $(\alpha, \alpha', \gamma)$ experiments in stable nuclei, may modify the shape of the energy distribution. The multistep contribution has been taken into account in ref. [50], for Coulomb relativistic excitation of Tin isotopes, where this effect has been estimated for the ^{132}Sn to be of the order of 10%. In order to further improve this observation, we are planning a new experiment to excite the pygmy dipole resonance with both isoscalar and isovector probes.

Acknowledgements

Special thanks are due to the technical staff of the LNS cyclotron and especially the head of accelerator division G. Cosentino for the production of the fragmentation beam. A particular mention for the help in the understanding of the transmission of different charge status of the beam is due to C. Nociforo of GSI, Darmstadt. We also thank M.H. Harakeh for the fruitful suggestions.

References

[1] N. Paar, et al., Rep. Prog. Phys. C 70 (2007) 691 and references therein.
[2] D. Savran, et al., Prog. Part. Nucl. Phys. 70 (2013) 210–245.
[3] A. Bracco, et al., Eur. Phys. J. A 51 (2015) 99.
[4] F. Catara, et al., Nucl. Phys. A 624 (1997) 449–458.
[5] A. Klimkiewicz, et al., Phys. Rev. C 76 (2007) 051603.
[6] J. Piekarewicz, Phys. Rev. C 73 (2006) 044325.
[7] S. Goriely, E. Khan, Nucl. Phys. A 706 (2002) 217–232.
[8] N. Tsoneva, et al., Phys. Rev. C 91 (2015) 044318.
[9] E. Litvinova, et al., Nucl. Phys. A 823 (2009) 26–37.
[10] D. Vretenar, et al., Nucl. Phys. A 692 (2001) 496–517.
[11] N. Paar, et al., Phys. Lett. B 606 (2005) 288–294.
[12] E. Litvinova, et al., Phys. Lett. B 647 (2007) 111–117.
[13] N. Tsoneva, H. Lenske, Phys. Rev. C 77 (2008) 024321.
[14] E.G. Lanza, et al., Phys. Rev. C 79 (2009) 054615.
[15] E.G. Lanza, et al., Phys. Rev. C 84 (2011) 064602.
[16] E.G. Lanza, et al., Phys. Rev. C 91 (2015) 054607.
[17] D. Savran, et al., Phys. Rev. Lett. 97 (2006) 172502.
[18] X. Roca-Maza, et al., Phys. Rev. C 85 (2012) 024601.
[19] D. Savran, et al., Phys. Rev. C 84 (2011) 024326.
[20] V. Derya, et al., Phys. Lett. B 730 (2014) 288–292.
[21] F.C.L. Crespi, et al., Phys. Rev. Lett. 113 (2014) 012501.
[22] L. Pellegri, et al., Phys. Lett. B 738 (2014) 519–523.
[23] M. Krzysiek, et al., Phys. Rev. C 93 (2016) 044330.
[24] F.C.L. Crespi, et al., Phys. Rev. C 91 (2015) 024323.
[25] D. Negi, et al., Phys. Rev. C 94 (2016) 024332.
[26] N. Nakatsuka, et al., Phys. Lett. B 768 (2017) 387–392.
[27] J. Endres, et al., Phys. Rev. C 80 (2009) 034302.
[28] P. Adrich, et al., Phys. Rev. Lett. 95 (2005) 132501.
[29] O. Wieland, et al., Phys. Rev. Lett. 102 (2009) 092502.
[30] D.M. Rossi, et al., Phys. Rev. Lett. 111 (2013) 242503.
[31] A. Leistenschneider, et al., Phys. Rev. Lett. 86 (2001) 5442–5445.
[32] E. Tryggestad, et al., Phys. Lett. B 541 (2002) 52–58.
[33] J. Gibelin, et al., Phys. Rev. Lett. 101 (2008) 212503.
[34] https://www.lns.infn.it/it/acceleratori/fribs-lns.htm, 2018.
[35] G. Raciti, et al., Nucl. Instrum. Methods B 266 (2008) 4632–4636.
[36] I. Lombardo, et al., Nucl. Phys. B, Proc. Suppl. 215 (2011) 272–274.
[37] E.V. Pagano, et al., EPJ Web Conf. 117 (2016) 10008.
[38] L. Acosta, et al., J. Phys. Conf. Ser. 730 (2016) 012001.
[39] A. Pagano, et al., Nucl. Phys. A 734 (2004) 504–511.
[40] A. Pagano, Nucl. Phys. News 22 (2012) 25–30.
[41] M. Alderighi, et al., Nucl. Instrum. Methods A 489 (2002) 257–265.
[42] G. Cardella, et al., Nucl. Instrum. Methods A 799 (2015) 64–69.
[43] G. Cardella, et al., EPJ Web Conf. 165 (2017) 01009.
[44] F. Puhlhofer, Nucl. Phys. A 280 (1977) 267–284.
[45] I. Dioszegi, Phys. Rev. C 64 (2001) 019801.
[46] M. Vandebrouck, et al., Phys. Rev. Lett. 113 (2014) 032504.
[47] M. Vandebrouck, et al., Phys. Rev. C 92 (2015) 024316.
[48] D. Kresan, et al., J. Phys. Conf. Ser. 523 (2014) 012034.
[49] S. Agostinelli, et al., Nucl. Instrum. Methods A 506 (2003) 250–303.
[50] E.G. Lanza, et al., Phys. Rev. C 79 (2009) 054615.